

2052 3.4 Solutions of Exercises of Chapter 3: Classical Cyclotron

2053 3.1 Modeling a Cyclotron Dipole: Using a Field Map

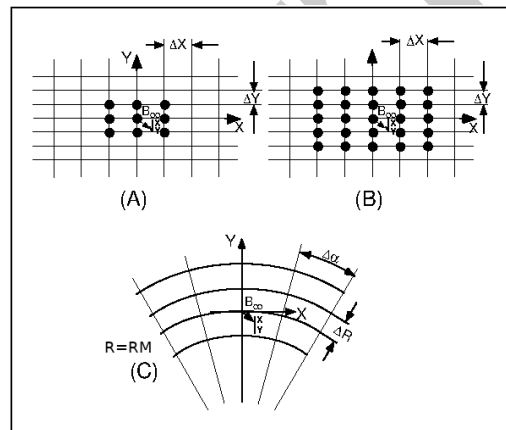
2054

2055 (a) A field map of a 180° sector of a classical cyclotron magnet.

2056 The first option is retained here: a Fortran program, `geneSectorMap.f`, given in
 2057 Tab. 3.1. constructs the required map of a field distribution $B_Z(R, \theta)$, to be subse-
 2058 quently read and raytraced through using the keyword TOSCA [16, *lookup INDEX*].

2059 Regarding the second option: using the analytical model DIPOLE together with
 2060 the keyword OPTIONS[CONSTY=ON] to fabricate a field map, examples can be
 2061 found for instance in the FFAG chapter exercises (Chap. 10).

Fig. 3.19 Principle 2-D field map mesh as used by TOSCA, and the (O;X,Y) coordinate system. (A), (B): Cartesian mesh in the (X,Y) plane, case of respectively 9-point and a 25-point interpolation grid; the mesh increments are ΔX and ΔY . (C) : polar mesh and increments ΔR and $\Delta \alpha$ ($\Delta \theta$ in the text), and (O;X,Y) frame moving along a reference arc of radius R_M . The field at particle location is interpolated from its values at the closest 3×3 or 5×5 nodes



2062 A polar mesh is retained (Fig. 3.19), rather than Cartesian, consistently with
 2063 cyclotron magnet symmetry. The program can be compiled (`gfortran -o geneSectorMap geneSectorMap.f` will provide the executable, `geneSectorMap`) and run, as
 2064 is. The field map is saved under the name `geneSectorMap.out`, excerpts of the expected content are given in Tab. 3.2. That name appears under TOSCA in `zgoubi`
 2065 input data file for this simulation (Tab. 3.3). Figure 3.20 shows the field over the
 2066 180° azimuthal extent (using a gnuplot script, bottom of Tab. 3.2).

2067 Note the following:

2068 (i) the field map azimuthal extent (set at 180° in `geneSectorMap`) can be changed,
 2069 for instance to simulate a 60 deg sector instead;

2070 (ii) the field is vertical being the mid-plane field of dipole magnet. The field
 2071 is taken constant in this exercise, $\forall R, \forall \theta$ throughout the map mesh, whereas in
 2072 upcoming exercises, a *focusing index* will be introduced, which will make $B_Z \equiv$
 2073 $B_Z(R)$ an R-dependent quantity (in Chap. 4 which addresses Thomas focusing and
 2074 the isochronous cyclotron, exercises will further resort to $B_Z \equiv B_Z(R, \theta)$, an R- and
 2075 θ -dependent quantity).

Table 3.1 A Fortran program which generates a 180° mid-plane field map. This angle as well as field amplitude can be changed, a field index can be added. This program can be compiled and run, as is. The field map it produces is logged in geneSectorMap.out

```

C geneSectorMap.f program
  implicit double precision (a-h,o-z)
  parameter (pi=4.d0*atan(1.d0), BY=0.d0, BX=0.d0, Z=0.d0)

  open(unit=2,file='geneSectorMap.out')           ! Field map storage file.

C----- Hypotheses :
  AT = 180.d0 /180.d0*pi           ! Angular extent of field map. Can be changed 360, 60 deg, etc.).
  BZ=5.d0                          ! Field (kG).
  Rmi=1.d0; Rma=76.d0; RM=50.d0    ! cm. Radial extent of field map; reference radius to define mesh.
  dR = 0.5d0 ; NR = NINT((Rma - Rmi)/dR)+1 ! R-distance between nodes in mesh. Number of R-nodes.
C                                     RdA=RM*dA is the distance between two nodes along R=RM arc.
  RdA = 0.5d0 ! given angle increment dA (dA is the "Delta theta" quantity in the main text).
  NX= NINT(RM*AT /RdA) +1 ; RdA= RM*AT / DBLE(NX -1) ! exact mesh step at RM, corresponding to NX.
  dA = RdA / RM ; A1 = 0.d0 ; A2 = AT           ! corresponding delta_angle.
C-----
  write(2,*) Rmi,dR,pi*pi*180.d0,dZ,
  >' ! Rmi/cm, dR/cm, dA/deg, dZ/cm'
  write(2,*) '# Field map generated using geneSectorMap.f '
  write(2,fmt='(a)') '# AT/rd, AT/deg, Rmi/cm, Rma/cm, RM/cm,'
  >/' NR, dR/cm, NX, RdA/cm, dA/rd : '
  write(2,fmt='(a,1p,5(e16.8,1x),2(i3,1x,e16.8,1x),e16.8)')
  >' # ,AT, AT/pi*180.d0,Rmi, Rma, RM, NR, dR, NX, RdA, dA
  write(2,*) '# For TOSCA: ',NX,NR,' 1 22.1 1. ! IZ=1 -> 2D ; '
  >/' MOD=22 -> polar map ; .MOD2=-1 -> one map file'
  write(2,*) '# R*cosA Z=0, R*sinA'
  >/' BY BZ BX ix jr'
  write(2,*) '# cm cm cm '
  >/' kG kG kG '
  write(2,*) '# '
  do jr = 1, NR
    R = Rmi + dble(jr-1)*dR
    do ix = 1, NX
      A = A1 + dble(ix-1)*dA ; X = R * sin(A) ; Y = R * cos(A)
      write(2,fmt='(1p,6(e16.8),2(1x,i0))') Y,Z,X,BY,BZ,BX,ix,jr
    enddo
  enddo
  stop ' Job complete ! Field map stored in geneSectorMap.out.'
  end

```

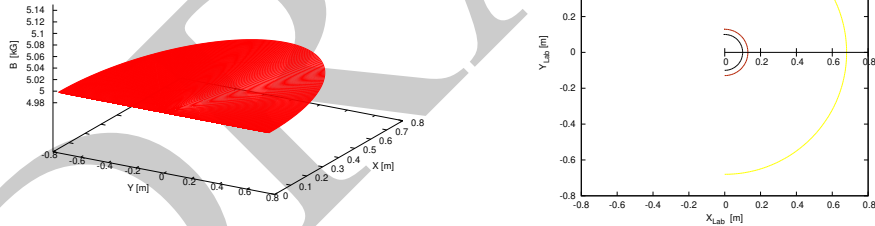


Fig. 3.20 Left: map of a constant magnetic field over a 180 deg sector, 76 cm radial extent. Right: three circular trajectories, at respectively 0.12, 0.2 and 5.52 MeV, computed using that field map

Table 3.2 First and last few lines of the field map file `geneSectorMap.out`. The file starts with an 8-line header, the first of which is effectively used by `zgoubi` (the following 7 are not used) and indicates, in that order: the minimum radius of the map mesh R_{mi} , the radial increment dR , the azimuthal increment dA , the axial increment dZ (null and not used in the present case of a two-dimensional field map), in units of, respectively, cm, cm, degree, cm. The additional 7 lines provide the user with various indications regarding numerical values used in, or resulting from, the execution of `geneSectorMap.f`. The first 5 numerical data in line 5 in particular are to be reported in `zgoubi` input data file under TOSCA keyword. The rest of the file is comprised of 8 columns, the first three give the node coordinates and the next three the field component values at that node, the last two columns are the (azimuthal and radial) node numbers, from (1,1) to (315,151) in the present case

```

1.00      0.500      0.57324840764331209      0.00      ! Rmi/cm, dR/cm, dA/deg, dZ/cm
# Field map generated using geneSectorMap.f
# AT/rd, AT/deg, Rmi/cm, Rma/cm, RM/cm, NR, dR/cm, NX, RdA/cm, dA/rd :
# 3.14159265E+00 1.800E+02 1.000E+00 7.600E+01 5.000E+01 151 5.000E-01 315 5.00253607E-01 1.00050721E-02
# For TOSCA:      315      151 1 22.1 1. !IZ=1 -> 2D; MOD=22 -> polar map; .MOD2=-1 -> one map file
#
# R*cosA      Z=0,      R*sinA      BY      BZ      BX      ix jr
# cm          cm          cm          kG          kG          kG
1.00000000E+00 0.00000000E+00 0.00000000E+00 0.00000000E+00 5.00000000E+00 0.00000000E+00 1 1
9.99949950E-01 0.00000000E+00 1.00049052E-02 0.00000000E+00 5.00000000E+00 0.00000000E+00 2 1
9.99799804E-01 0.00000000E+00 2.00088090E-02 0.00000000E+00 5.00000000E+00 0.00000000E+00 3 1
9.99549577E-01 0.00000000E+00 3.00107098E-02 0.00000000E+00 5.00000000E+00 0.00000000E+00 4 1
9.99199295E-01 0.00000000E+00 4.00096065E-02 0.00000000E+00 5.00000000E+00 0.00000000E+00 5 1
9.99199295E-01 0.00000000E+00 4.00096065E-02 0.00000000E+00 5.00000000E+00 0.00000000E+00 5 1
.....
-7.59391464E-01 0.00000000E+00 3.04073010E+00 0.00000000E+00 5.00000000E+00 0.00000000E+00 311 151
-7.59657679E-01 0.00000000E+00 2.28081394E+00 0.00000000E+00 5.00000000E+00 0.00000000E+00 312 151
-7.59847851E-01 0.00000000E+00 1.52066948E+00 0.00000000E+00 5.00000000E+00 0.00000000E+00 313 151
-7.59961962E-01 0.00000000E+00 7.60372797E-01 0.00000000E+00 5.00000000E+00 0.00000000E+00 314 151
-7.60000000E+01 0.00000000E+00 9.30731567E-15 0.00000000E+00 5.00000000E+00 0.00000000E+00 315 151

```

A *gnuplot* script to obtain a graph of $B(X,Y)$, Fig. 3.20:

```

# gnuplot_fieldMap.gnu
set key maxcol 1 ; set key t l ; set xtics mirror ; set ytics mirror ; cm2m = 0.01
set xlabel "Y [m]"; set ylabel "X [m]"; set zlabel "B [kG] \n" rotate by 90; set zrange [:5.15]
splot "geneSectorMap.out" u ($1 * cm2m):($3 * cm2m):($5) w l lc rgb "red" notit; pause 1

```

2078 This field map can be readily tested using the example of Tab. 3.3, which raytraces
2079 $E_k = 0.12, 0.2$ and 5.52 MeV protons on circular trajectories centered at the center
2080 of the field map. Trajectory radii, respectively $R = 10.011, 12.924$ and 67.998 cm
2081 (Tab. 3.3), have been prior determined from

$$\text{Rigidity } B\rho = B_0 \times R \quad \text{and} \quad B\rho = p/c = \sqrt{E_k(E_k + 2M)}/c \quad (3.34)$$

2082 with $B_0 = 0.5$ T (Tab. 3.1) and $M = 938.272$ MeV/ c^2 the proton mass.

2083 The optical sequence for this particle raytracing uses the following keywords:

2084 (i) OBJET to define a (arbitrary) reference rigidity and initial particle coordinates

2085 (ii) TOSCA, to read the field map and raytrace through (and TOSCA's 'IL=2'

2086 flag to store step-by-step particle data into `zgoubi.plt`)

2087 (iii) FAISCEAU to print out particle coordinates in `zgoubi.res` execution listing

2088 (iv) SYSTEM to run a `gnuplot` script (Tab. 3.3) once raytracing is complete

2089 (v) MARKER, to define two particular "LABEL_1" type labels [16, *lookup INDEX*]

2090 (`#S_halfDipole` and `#E_halfDipole`), to be used with `INCLUDE` in subsequent exer-

2091 cises.

Table 3.3 Simulation input data file FieldMapSector.inc: it is set to allow a preliminary test regarding the field map geneSectorMap.out (as produced by the Fortran program geneSectorMap, Tab. 3.1), by computing three circular trajectories centered on the center of the map. This file also defines the INCLUDE segment between the labels (LABEL1 type [16, Sect. 7.7]) #S_halfDipole and #E_halfDipole

```

FieldMapSector.inc
! Uniform field 180 deg sector. FieldMapSector.inc.
'MARKER' FieldMapSector_S ! Just for edition purposes.
'OBJET'
64.62444403717985 ! Reference Brho ("BORO" in the users' guide) -> 200keV proton.
2
3 1
10.011362 0. 0. 0. 0.7745802 'a' ! p[MeV/c]= 15.007, Brho[kG.cm]= 50.057, kin-E[MeV]=0.12.
12.924888 0. 0. 0. 1. 'b' ! kin-E[MeV]=0.2.
67.997983 0. 0. 0. 5.2610112 'c' ! p[MeV/c]=101.926, Brho[kG.cm]=339.990, kin-E[MeV]=5.52.
1 1 1
'MARKER' #S_halfDipole
'TOSCA'
0 2 ! IL=2 to log step-by-step coordinates, spin, etc., to zgoubi.plt (avoid, if CPU time matters).
1. 1. 1. 1. ! Normalization coefficients, for B, X, Y and Z coordinate values read from the map.
HEADER_8 ! The field map file starts with an 8-line header.
315 151 1 22.1 1. ! IZ=1 for 2D map; MOD=22 for polar frame; .MOD2=.1 if only one map file.
geneSectorMap.out
0 0 0 0 ! Possible vertical boundaries within the field map, to start/stop stepwise integration.
2
1. ! Integration step size. Small enough for orbits to close accurately.
2 ! Magnet positioning option.
0. 0. 0. 0. ! Magnet positioning.
'MARKER' #E_halfDipole
'FAISCEAU'
'SYSTEM' ! This SYSTEM command runs gnuplot, for a graph of the two trajectories.
1
gnuplot <./gnuplot_Zplt.gnu
'MARKER' FieldMapSector_E ! Just for edition purposes.
'END'

```

A gnuplot script to obtain a graph of the orbits, Fig. 3.20:

```

# gnuplot_Zplt.gnu
set key maxcol 1 ; set key t r ; set xtics ; set ytics ; cm2m = 0.01 ; unset colorbox
set xlabel "X_{Lab} [m]" ; set ylabel "Y_{Lab} [m]" ; set size ratio 1 ; set polar
plot for [orbit=1:3] "zgoubi.plt" u ($19==orbit ? $22 :1/0):($10 *cm2m):($19 w l lw 2 lc pal; pause 1

```

2092 Three circular trajectories in a dee, resulting from the data file of Tab. 3.3 are
 2093 shown in Fig. 3.20. Inspecting zgoubi.res execution listing one finds the D, Y, T, Z,
 2094 P, S particle coordinates under FAISCEAU, at OBJET (left) and current (right) after
 2095 a turn in the cyclotron (unchanged, as the trajectory forms a closed orbit):

```

2096      6 Keyword, label(s) : FAISCEAU IPASS= 1
2097
2098      TRACE DU FAISCEAU
2099      (follows element # 5)
2100      2 TRAJECTOIRES
2101
2102      OBJET
2103      D Y(cm) T(mr) Z(cm) P(mr) S(cm) D-1 Y(cm) T(mr) Z(cm) P(mr) S(cm)
2104      o 1 0.7746 10.011 0.000 0.000 0.000 0.0000 -0.2254 10.011 -0.000 0.000 0.000 3.145152E+01 1
2105      o 1 5.2610 67.998 0.000 0.000 0.000 0.0000 4.2610 67.998 -0.000 0.000 0.000 2.136220E+02 2

```

2104 (b) Concentric trajectories in the median plane.

2105 The optical sequence for this exercise is given in Tab. 3.4. Compared to the
 2106 previous sequence (Tab. 3.3), (i) the TOSCA segment has been replaced by an
 2107 INCLUDE, for the mere interest of making the input data file for this simulation
 2108 shorter, and (ii) additional keywords are introduced, including

- 2109 - FIT, which finds the circular orbit for a particular momentum,
- 2110 - FAISCEAU, a means to check local particle coordinates,

Table 3.4 Simulation input data file: optical sequence to find cyclotron closed orbits at a series of different momenta. An INCLUDE inserts the #S_halfDipole to #E_halfDipole TOSCA segment of the sequence of Tab. 3.3

```

Uniform field 180 deg. sector. Find orbits.
'MARKER' FieldMapOrbits_S                               ! Just for edition purposes.
'OBJET'
64.62444403717985                                     ! Reference Brho ("BORO" in the users' guide) -> 200keV proton.
2
1 1                                                    ! Just one ion.
12.9248888074 0. 0. 0. 0. 1. 'm'                    ! This initial radius yields BR=64.6244440372 kg.cm.
1
'INCLUDE'                                             ! A half of the cyclotron dipole.
1
FieldMapSector.inc[#S_halfDipole:#E_halfDipole]
'FAISCEAU'
'INCLUDE'                                             ! A half of the cyclotron dipole.
1
FieldMapSector.inc[#S_halfDipole:#E_halfDipole]
'FIT'
1
2 35 0 6.                                             ! Vary momentum, to allow fulfilling the following constraint:
1
3.1 1 2 5 0. 1. 0                                     ! request same radius after a half-turn (i.e., after first 180 deg sector,
! this ensures centering of orbit on center of map).
'FAISCEAU' CHECK ! Allows quick check of particle coordinates, in zgoubi.res: final should = initial.

'REBELOTE'                                           ! Repeat what precedes,
15 0.1 0 1                                           ! 15 times.
1
OBJET 30 10:80 ! Prior to each repeat, first change the value of parameter 30 (i.e., Y) in OBJET.
'SYSTEM'
2
gnuplot <./gnuplot_Zplt.gnu
cp gnuplot_Zplt_XYLab.eps gnuplot_Zplt_XYLab_stage1.eps
'MARKER' FieldMapOrbits_E                               ! Just for edition purposes.
'END'

```

A *gnuplot* script to obtain Fig. 3.21:

Note: removing the test '\$51==1 ?' on column 51 in *zgoubi.plt*, would add on the graph the orbit as it is before each FIT.

```

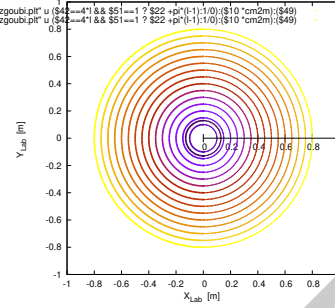
# gnuplot_Zplt.gnu
set key maxcol 1 ; set key t r ; set xtics ; set ytics ; set size ratio 1 ; set polar ; unset colorbox
set xlabel "X_{Lab} [m] \n" ; set ylabel "Y_{Lab} [m] \n" ; cm2m = 0.01 ; sector1=4 ; sector2=8 ; pi = 4.*atan(1.)
lmnt1 = 4 ; lmnt2=8 ## column numer in zgoubi.plt, $42: NOEL; $51: FITLST; $49: FIT number
plot for [l=lmnt1/4:lmnt2/4] "zgoubi.plt" u ($42==4*1 && $51==1 ? $22 +pi*(1-1):1/0):(510 *cm2m):(549) w p ps .3 lc pal
pause 1

```

2111 - REBELOTE, which repeats the execution of the sequence (REBELOTE sends
 2112 the execution pointer back to the top of the data file) for a new momentum value
 2113 which REBELOTE itself defines, prior.

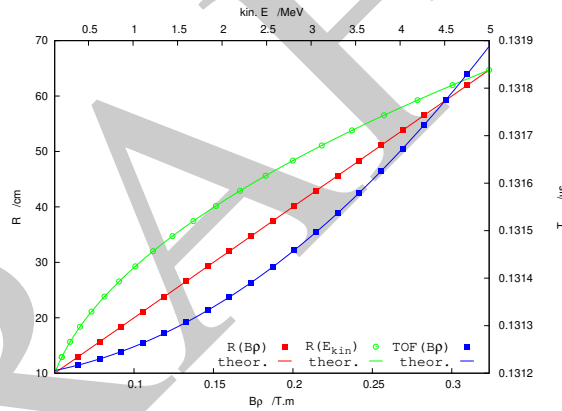
2114 In order to compute and then plot trajectories (Fig. 3.21), *zgoubi* proceeds as
 2115 follows: orbit circles for a series of different radii taken in [10, 80] cm are searched,
 2116 using FIT to find the appropriate momenta. REBELOTE is used to repeat that fitting
 2117 on a series of different values of R; prior to repeating, REBELOTE modifies the
 2118 initial particle coordinate Y_0 in OBJET. Stepwise particle data through the dipole
 2119 field are logged in *zgoubi.plt*, due to IL=2 under TOSCA keyword, at the first pass
 2120 before FIT, and at the last pass following FIT completion. A key point here: a flag,
 2121 FITLST, recorded in column 51 in *zgoubi.plt* [16, Sect.8.3], is set to 1 at the last
 2122 pass (the last pass follows the completion of the FIT execution and uses updated FIT
 2123 variable values).

Fig. 3.21 Circular trajectories in the cyclotron mid-plane, centered on the field map center. The outermost orbit is at $R=80$ cm by hypothesis, thus $BR = B_0 \times R = 0.4$ Tm, $E_k = 7.632$ MeV. These stepwise (R, θ) data are read from `zgoubi.plt`, coordinates (Y, X) in `zgoubi` polar frame nomenclature [16, Sect.8.3]



2124 At the bottom of `zgoubi` input data file, a `SYSTEM` command produces a graph
 2125 of ion trajectories, by executing a `gnuplot` script (bottom of Tab. 3.4). Note the test
 2126 on `FITLST`, which allows selecting the last pass following `FIT` completion. Graphic
 2127 outcomes are given in Fig. 3.21.

Fig. 3.22 Numerical (markers) and theoretical (solid lines) values of orbit radius, R , and revolution period, T_{rev} , versus kinetic energy (top scale) and rigidity (bottom scale). The mesh density here is $N_\theta \times N_R = 315 \times 151$. The integration step size is $\Delta s = 1$ cm, so ensuring converged results (to $\Delta R/R$ and $\Delta T_{rev}/T_{rev} < 10^{-6}$)



2128 The reason why it is possible to push the raytracing beyond the 76 cm radius field
 2129 map extent, without loss of accuracy, is that the field is constant. Thus, referring to
 2130 the polynomial interpolation technique used [16, Sect. 1.4], the extrapolation out of
 2131 the map will leave the field value unchanged.

2132 (c) Energy and rigidity dependence of orbit radius and time-of-flight.

2133 The orbit radius R and the revolution time T_{rev} as a function of kinetic energy E_k
 2134 and rigidity BR are obtained by a similar scan to exercise (b). The results are shown
 2135 in Fig. 3.22.

2136 A slow increase of revolution period with energy can be observed, which is due
 2137 to the mass increase.

2138 Note that these results are converged for the step size, to high accuracy (see (d)),
 2139 due to its value taken small enough, namely $\Delta s = 1$ cm. This corresponds for instance
 2140 to 80 steps to complete a revolution for the 120 keV, $R = 12.9$ cm smaller radius
 2141 trajectory in Fig 3.21.

Fig. 3.23 Convergence versus mesh density and step size: a graph of orbit radius R (left axis), and revolution period, T_{rev} (right axis), versus kinetic energy (top scale) and rigidity (bottom scale). Solid markers are for $\Delta s = 1$ cm and $N_\theta \times N_R = 3 \times 3$ node mesh, large empty circles are for $\Delta s = 10$ cm and $N_\theta \times N_R = 106 \times 151$ node mesh. Solid lines are from theory and show convergence in the case 3×3 nodes and $\Delta s = 1$ cm

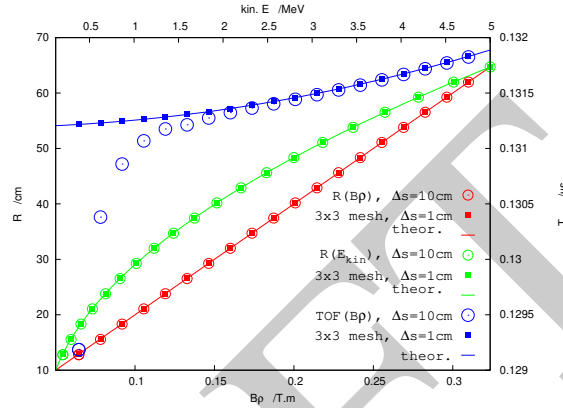


Table 3.5 Field map of a 60° constant field sector as read by TOSCA. The field map is complete, with smallest possible $NX \times NR = 3 \times 3 = 9$ number of nodes. The first line of the header is used by zgoubi (the following 7 are not used), namely, the minimum value of the radius in the map, radius increment, azimuthal increment, and vertical increment (null here, as this is a single, mid-plane map)

```

1.0 37.50 30.0 0. ! Rmi/cm, dR/cm, dA/deg, dZ/cm
# Field map generated using geneSectorMap.f
# AT/rd, AT/deg, Rmi/cm, Rma/cm, RM/cm, NR, dR/cm, NX, RdA/cm, dA/rd :
# 1.04719755E+00 60. 1. 76. 50. 3 37.5 3 26.1799388 0.523598776
# For TOSCA: 3 3 1 22.1 1. !IZ=1 -> 2D ; MOD=22 -> polar map ; .MOD2=-1 -> one map file
#
# R*cosA Z=0, R*sinA BY BZ BX ix jr
# cm cm cm kG kG kG kG
1.00000000E+00 0.00000000E+00 0.00000000E+00 0.00000000E+00 5.00000000E+00 0.00000000E+00 1 1
8.66025404E-01 0.00000000E+00 5.00000000E-01 0.00000000E+00 5.00000000E+00 0.00000000E+00 2 1
5.00000000E-01 0.00000000E+00 8.66025404E-01 0.00000000E+00 5.00000000E+00 0.00000000E+00 3 1
3.85000000E-01 0.00000000E+00 0.00000000E+00 0.00000000E+00 5.00000000E+00 0.00000000E+00 1 2
3.33419780E-01 0.00000000E+00 1.92500000E+01 0.00000000E+00 5.00000000E+00 0.00000000E+00 2 2
1.92500000E-01 0.00000000E+00 3.33419780E+01 0.00000000E+00 5.00000000E+00 0.00000000E+00 3 2
7.60000000E-01 0.00000000E+00 0.00000000E+00 0.00000000E+00 5.00000000E+00 0.00000000E+00 1 3
6.58179307E-01 0.00000000E+00 3.80000000E+01 0.00000000E+00 5.00000000E+00 0.00000000E+00 2 3
3.80000000E-01 0.00000000E+00 6.58179307E+01 0.00000000E+00 5.00000000E+00 0.00000000E+00 3 3

```

Modified TOSCA keyword data, in the case of a 60° sector field map (compared to Tab. 3.3, the sole data line “3 3 1 22.1 1.” changes, from “315 151 1 22.1 1.” in that earlier 180° sector case):

```

'TOSCA'
0 2 ! IL=2: log step-by-step coordinates, spin, etc., in zgoubi.plt (avoid if CPU time matters).
1. 1. 1. 1. ! Normalization coefficients, for B, X, Y and Z coordinate values read from the map.
HEADER_8 ! The field map file starts with an 8-line header.
3 3 1 22.1 1. ! IZ=1 for 2D map; MOD=22 for polar frame; .MOD2=-1 if only one map file.
geneSectorMap.out
0 0 0 0 ! Possible vertical boundaries within the field map, to start/stop stepwise integration.
2
1. ! Integration step size. Small enough for orbits to close accurately.
2 ! Magnet positioning option.
0. 0. 0. 0. ! Magnet positioning.

```

2142 (d) Numerical convergence: mesh density.

2143 This question concerns the dependence of the numerical convergence of the
2144 solution of the differential equation of motion [16, Eq. 1.2.1] upon mesh density.

2145 The program used in (b) to generate a field map (Tab. 3.1) is modified to construct
2146 field maps of $B_Z(R, \theta)$ with various radial and azimuthal mesh densities. Changing
2147 these is simply a matter of modifying the quantities dR (radius increment ΔR) and
2148 $R dA$ (R times the azimuth increment $\Delta\theta$) in the program of Tab. 3.1. The field maps
2149 `geneSectorMap.out` so generated for various (dR, RdA) couples may be saved under
2150 different names, and used separately.

2151 Table. 3.5 shows the complete, 9 line, TOSCA field map, in the case of a 60°
2152 sector covered in $N_\theta \times N_R = \frac{60^\circ}{\Delta\theta} \times \frac{75 \text{ cm}}{\Delta R} = \frac{360^\circ}{120^\circ} \times \frac{75 \text{ cm}}{37.5 \text{ cm}} = 3 \times 3$ nodes. Six
2153 sectors are now required to cover the complete cyclotron dipole: `zgoubi` input data
2154 need be changed accordingly, namely stating TOSCA - possibly via an `INCLUDE` -
2155 six times, instead of just twice in the case of a 180 degree sector.

2156 The result to be expected: with a mesh reduced to as low as $N_\theta \times N_R = 3 \times 3$,
2157 compared to $N_\theta \times N_R = 106 \times 151$, radius and time-of-flight should however remain
2158 unchanged. This shows in Fig. 3.23 which displays both cases, over a $E_k : 0.12 \rightarrow$
2159 5 MeV energy span (assuming protons). The reason for the absence of effect of the
2160 mesh density is that the field is constant. As a consequence the field derivatives in the
2161 Taylor series based numerical integrator are all zero [16, Sect. 1.2]: only B_Z is left
2162 in evaluating the Taylor series, however B_Z is constant. Thus R remains unchanged
2163 when pushing the ion by a step Δs , and the cumulated path length - the closed orbit
2164 length - and revolution time - path length over velocity - end up unchanged. Note:
2165 this will no longer be the case when a radial field index is introduced in order to
2166 cause vertical focusing, in subsequent exercises.

2167 (e) Numerical convergence: integration step size

2168 Figure 3.23 displays two cases of step sizes, $\Delta s \approx 1 \text{ cm}$ and $\Delta s = 10 \text{ cm}$.

2169 It has been shown (Fig. 3.22) that $\Delta s \approx 1 \text{ cm}$ is small enough that the numerical
2170 integration is converged, agreement with theoretical expectation is quite good.

2171 The difference on the value of R , in the case $\Delta s \approx 10 \text{ cm}$, appears to be weak,
2172 only noticeable at the scale of the graph for R values small enough that the number
2173 of steps over one revolution goes as low as $2\pi R/\Delta s \approx 2\pi \times 14.5/10 \approx 9$. The change
2174 in time-of-flight due to the larger step size amounts to a relative 10^{-3} .

2175 Step size is critical in the numerical integration, the reason is that the coefficients
2176 of the Taylor series that yield the new position vector $\mathbf{R}(M_1)$ and velocity vector
2177 $\mathbf{v}(M_1)$, from an initial location M_0 after a Δs push, are the derivatives of the velocity
2178 vector [16, Sect. 1.2] and may take substantial values if $\mathbf{v}(s)$ changes quickly. In
2179 such case, taking too large a Δs value makes the high order terms significant and
2180 the Taylor series truncation [16, Eq. 1.2.4] is fatal to the accuracy (regardless of a
2181 possible additional issue of radius of convergence of the series).

2182 (f) Numerical convergence: $\frac{\delta R}{R}(\Delta s)$

2183 Issues faced are the following:

2184 - the increase of $\delta R(\Delta s)/R$ at large Δs has been addressed above;

2185 - a small Δs is liable to cause an increase of $\delta R(\Delta s)/R$, due to computer accuracy:
2186 truncation of numerical values at a limited number of digits may cause a Δs push to
2187 result in no change in $\mathbf{R}(M_1)$ (position) and $\mathbf{u}(M_1)$ (normed velocity) quantities [16,
2188 Eq. 1.2.4].

2189 A detailed answer to the question, including graphs, is left to the reader, the
2190 method is the same as in (e).

DRAFT

2191 **3.2 Modeling a Cyclotron Dipole: Using an Analytical Field Model**

2192

2193 This exercise introduces the analytical modeling of a dipole, using DIPOLE [16,
2194 *lookup* INDEX], and compares outcomes to the field map case of exercise 3.1. The
2195 exercise is not entirely solved, however all the material needed for that is provided,
2196 and indications are given to complete it.

2197 (a) Analytical modeling.

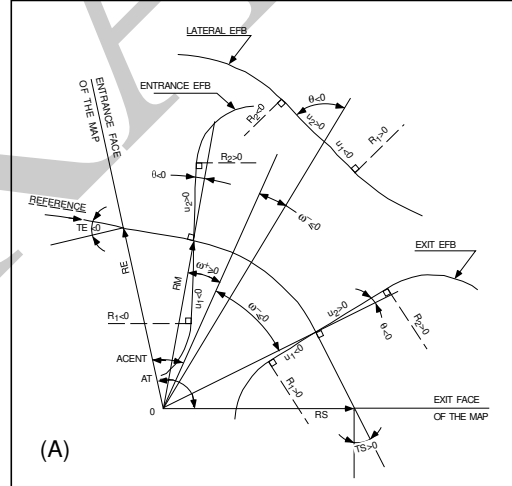
2198 DIPOLE keyword provides an analytical model of the field to simulate a sector
2199 dipole with index, namely [16, *lookup* INDEX]

$$B_Z = \mathcal{F}(\theta) B_0 \left[1 + k \left(\frac{R - R_0}{R_0} \right) + k' \left(\frac{R - R_0}{R_0} \right)^2 + k'' \left(\frac{R - R_0}{R_0} \right)^3 \right] \quad (3.35)$$

2200 R_0 is a reference radius, $B_0 = B_Z(R_0)|_{\mathcal{F}=1}$ is a reference field value, k is the field
2201 index and k' , k'' are homogeneous to its first and second derivative with respect to
2202 R (Eq. 3.11). $\mathcal{F}(\theta)$ is an azimuthal form factor, defined by the fringe field model,
2203 presumably taking the value 1 in the body of the dipole. In the present case a
2204 hard-edge field model is considered, so that

$$\mathcal{F} = \begin{cases} 1 & \text{inside} \\ 0 & \text{outside} \end{cases} \text{ the dipole magnet} \quad (3.36)$$

Fig. 3.24 Parameters used to define the geometry of a dipole magnet with index, using DIPOLE. In the text, ACENT is noted ACN [16, Fig. 9]



2205 Setting up the input data list under DIPOLE (Table 3.6) requires close inspection
2206 of Fig. 3.24, which details the geometrical parameters such as the full angular
2207 opening of the field region that DIPOLE comprises, AT; a reference angle ACN

2208 to allow positioning the effective field boundaries at ω^+ and ω^- ; field and indices;
 2209 fringe field regions at $ACN - \omega^+$ (entrance) and $ACN - \omega^-$ (exit); wedge angles,
 2210 etc.

2211 A 60 deg sector is used here for convenience, it is detailed in Table 3.6 (Table 3.7
 2212 provides the definition of a 180 deg sector, for possible comparisons with the present
 2213 three-sector assembly).

2214 In setting up DIPOLE data the following values have been accounted for:

2215 - $R_0 = 50$ cm, an arbitrary value (consistent with other exercises), more or less
 2216 half the dipole extent,

2217 - $B_0 = B_Z(R_0) = 5$ kG, as in the previous exercise. Note in passing, $R_0 = 50$ cm
 2218 thus corresponds to $BR = 0.25$ T m, $E_k = 2.988575$ MeV proton kinetic energy,

2219 - radial field index $k = 0$ for the time being (constant field at all (R, θ)),

2220 - a hard-edge field model for \mathcal{F} (Eq. 3.36). In that manner for instance, two
 2221 consecutive 60 deg sectors form a continuous 120 deg sector.

2222 A graph of $B_Z(R, \theta)$ can be produced by computing constant radius orbits, for a
 2223 series of energies ranging in 0.12 – 5.52 MeV for instance. DIPOLE[IL=2] causes
 2224 logging of step by step particle data in zgoubi.plt, including particle position and
 2225 magnetic field vector; these data can be read and plotted, to yield similar results to
 2226 Fig. 3.20.

2227 (b) Concentric trajectories in the median plane.

2228 The optical sequence of Exercise 3.1-b (Tab. 3.4) can be used, by just changing
 2229 the INCLUDE to account for a 180° DIPOLE (instead of TOSCA), namely

```
2230 ' INCLUDE '
2231 1
2232 3* 60degSector.inc[#S_60degSectorUnifB:#E_60degSectorUnifB]
```

2233 wherein 60degSector.inc is the name of the data file of Tab. 3.6 and

2234 [#S_60degSectorUnifB:#E_60degSectorUnifB]

2235 is the DIPOLE segment as defined in the latter. Note that the segment represents a
 2236 60° DIPOLE, thus it is included 3 times.

2237 The additional keywords in that modified version of the Tab. 3.4 file include

2238 - FIT, which finds the circular orbit for a particular momentum,

2239 - FAISTORE to print out particle data once FIT is completed,

2240 - REBELOTE, which repeats the execution of the sequence (REBELOTE sends
 2241 the execution pointer back to the top of the data file) for a new momentum value
 2242 which REBELOTE itself defines.

2243 For the rest, follow the same procedure as for exercise 3.1-b. The results are the
 2244 same, Fig. 3.21.

2245 (c) Energy and rigidity dependence of orbit radius and time-of-flight.

2246 The orbit radius R and the revolution time T_{rev} as a function of kinetic energy E_k
 2247 and rigidity BR are obtained by a similar scan to exercise (b). The procedure is the
 2248 same as in exercise 3.1-c. Results are expected to be the same as well (Fig. 3.22).

2249 A comparison of revolution periods can be made using the simulation file of
 2250 Table 3.6 which happens to be set for a momentum scan and yields Fig. 3.25, to

2251 be compared to Fig. 3.22: DIPOLE and TOSCA produce the same results as long as
 2252 as both methods are converged, from the integration step size stand point (small
 2253 enough), and regarding TOSCA from field map mesh density stand point in addition
 2254 (dense enough).

2255 (d) Numerical convergence: integration step size; $\frac{\delta R}{R}(\Delta s)$.

2256 This question concerns the dependence of the numerical convergence of the
 2257 solution of the differential equation of motion upon integration step size.

2258 Follow the procedure of exercise 3.1-e: a similar outcome to Fig. 3.23 is expected
 2259 - ignoring mesh density with the present analytical modeling using DIPOLE.

2260 The $\frac{\delta R}{R}$ dependence upon the integration step size Δs is commented in exer-
 2261 cise 3.1-e and holds regardless of the field modeling method (field map or analytical
 2262 model).

2263 (e) Pros and cons.

2264 Using a field map is a convenient way to account for complicated one-, two- or
 2265 three-dimensional field distributions.

2266 However, using an analytical field model rather, ensures greater accuracy of the
 2267 integration method.

2268 CPU-time wise, one or the other method may be faster, depending on the problem.

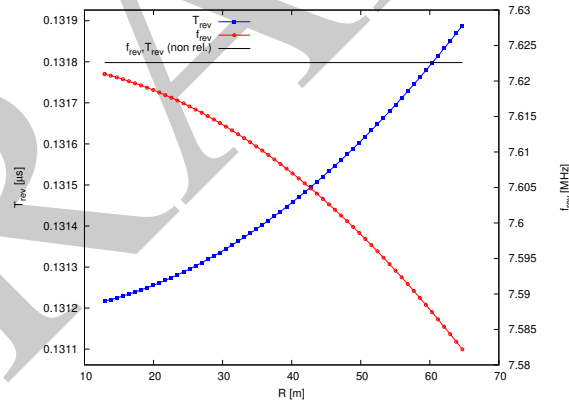


Fig. 3.25 A scan of radius-dependent revolution frequency. An analytical model of a cyclotron dipole is used, featuring uniform field (no radial gradient, at this point)

Table 3.6 Simulation input data file 60degSector.inc: analytical modeling of a dipole magnet, using DIPOLE. That file defines the labels (LABEL1 type [16, Sect. 7.7]) #S_60degSectorUnifB and #E_60degSectorUnifB, for INCLUDEs in subsequent exercises. It also realizes a 60-sample momentum scan of the cyclotron orbits, from 200 keV to 5 MeV, using REBELOTE

Note: this file is available in zgoubi sourceforge repository at

https://sourceforge.net/p/zgoubi/code/HEAD/tree/branches/exemples/book/zgoubiMaterial/cyclotron_classical/ProbMdlAnal/

```
60degSector.inc
! Cyclotron, classical. Analytical model of dipole field. File name: 60degSector.inc
'MARKER' ProbMdlAnal_S ! Just for edition purposes.
'OBJET'
64.62444403717985 ! 200keV proton.
2
1 1 ! Just one ion.
12.9248888074 0. 0. 0. 1. 'm' ! Closed orbit coordinates for D=p.p_0=1
1 ! => 200keV proton. R=Brho/B=64.624444037[kG.cm]/5[kG].
'PARTICUL' ! Optioanl - using PARTICUL is a way to get the time-of-flight computed.
PROTON ! otherwise, by default \zgoubi\ only requires rigidity.
'FAISCEAU' ! Local particle coordinates.
'MARKER' #S_60degSectorUnifB ! Label should not exceed 20 characters.
'DIPOLE' ! Analytical modeling of a dipole magnet.
2 ! IL=2, only purpose is to logged trajectories in zgoubi.plt, for further plotting.
60. 50. ! Sector angle AT; reference radius R0.
30. 5. 0. 0. 0. ! Reference azimuthal angle ACN; BM field at R0; indices, N, N', N''.
0. 0. ! EFB 1 is hard-edge.
4. .1455 2.2670 -.6395 1.1558 0. 0. 0. ! hard-edge only possible with sector magnet.
30. 0. 1.E6 -1.E6 1.E6 1.E6 ! Entrance face placed at omega+=30 deg from ACN.
0. 0. ! EFB 2.
4. .1455 2.2670 -.6395 1.1558 0. 0. 0.
-30. 0. 1.E6 -1.E6 1.E6 1.E6 ! Exit face placed at omega=-30 deg from ACN.
0. 0. ! EFB 3 (unused).
0. 0. 0. 0. 0. 0. 0. 0.
0. 0. 1.E6 -1.E6 1.E6 1.E6 0.
2 10 ! '2' is for 2nd degree interpolation. Could also be '25' (5*5 points grid) or 4 (4th degree).
1. ! Integration step size. Small enough for orbits to close accurately.
2 0. 0. 0. 0. ! Magnet positioning RE, TE, RS, TS. Could be instead non-zero, e.g.,
! 2 RE=50. 0. RS=50. 0., as long as Yo is amended accordingly in OBJET.
'MARKER' #E_60degSectorUnifB ! Label should not exceed 20 characters.
'FAISCEAU' ! Local particle coordinates.
'FIT' ! Adjust Yo at OBJET so to get final Y = Y0 -> a circular orbit.
1 nfinal
2 30 0 [12.,.65.] ! Variable : Yo.
1 2e-12 199 ! constraint; default penalty would be 1e-10; maximu 199 calls to function.
3.1 1 2 #End 0. 1. 0 ! Constraint: Y_final=Yo.
'FAISTORE' ! Log particle data here, to zgoubi.fai.
zgoubi.fai ! for further plotting (by gnuplot, below).
1
'REBELOTE' ! Momentum scan, 60 samples.
60 0.2 0 1 60 different rigidities; log to video ; take initial coordinates as found in OBJET.
1 ! Change parameter(s) as stated next lines.
OBJET 35 1:5.0063899693 ! Change relative rigity (35) in OBJET; range (0.2 MeV to 5 MeV).
'SYSTEM'
1 ! 2 SYSTEM commands follow.
/usr/bin/gnuplot < ./gnuplot_TOF.gnu & ! Launch plot by ./gnuplot_TOF.gnu.
'MARKER' ProbMdlAnal_E ! Just for edition purposes.
'END'
```

A gnuplot script, gnuplot_TOF.gnu, to obtain Fig. 3.25:

```
# gnuplot_TOF.gnu
set xlabel "R [m]"; set ylabel "T_{rev} [1/(\Symbol m)s]"; set y2label "f_{rev} [MHz]"
set xtics nomirror; set ytics nomirror; set y2tics nomirror; set key t l ; set key spacin 1.2
nSector=6; Hz2MHz=1e-6; M=938.272e6; c=2.99792458e8; B=0.5; freqNonRel(x)= Hz2MHz* c**2*B/M/(2.*pi)
set y2range [7.58:7.63] ; set yrange[1/7.63:1/7.58]
plot \
"zgoubi.fai" u 10:($15 *nSector) axes x1y1 w lp pt 5 ps .6 lw 2 linecolor rgb "blue" tit "T_{rev}" ,\
"zgoubi.fai" u 10:(1/($15*nSector)) axes x1y2 w lp pt 6 ps .6 lw 2 linecolor rgb "red" tit "f_{rev}" ,\
freqNonRel(x) axes x1y2 w l lw 2. linecolor rgb "black" tit "f_{rev},T_{rev} (non rel.)" ; pause 1
```

Table 3.7 A 180° version of a DIPOLE sector, where the foregoing quantities $AT = 60^\circ$, $ACN = \omega^+ = -\omega^- = 30^\circ$ have been changed to $AT = 180^\circ$, $ACN = \omega^+ = -\omega^- = 90^\circ$ - a file used under the name 180degSector.inc in further exercises

Note: this file is available in zgoubi sourceforge repository at

https://sourceforge.net/p/zgoubi/code/HEAD/tree/branches/exemples/book/zgoubiMaterial/cyclotron_classical/ProbMdlAnal/

```
! 180degSector.inc
'MARKER' #S_180degSectorUnifB ! Label should not exceed 20 characters.
'DIPOLE' ! Analytical modeling of a dipole magnet.
2
180. 50. ! Sector angle 180deg; reference radius 50cm.
90. 5. 0. 0. 0. ! Reference azimuthal angle; B0 field at R0; indices, N, N', N''.
0. 0. ! EFB 1 is hard-edge,
4 .1455 2.2670 -.6395 1.1558 0. 0. 0. ! hard-edge only possible with sector magnet.
90. 0. 1.E6 -1.E6 1.E6 1.E6 ! EFB 2.
0. 0. ! EFB 3.
4 .1455 2.2670 -.6395 1.1558 0. 0. 0.
-90. 0. 1.E6 -1.E6 1.E6 1.E6
0. 0. ! EFB 3.
0. 0. 0. 0. 0. 0. 0. 0.
0. 0. 1.E6 -1.E6 1.E6 1.E6 0.
2 10.
0.5 ! Integration step size. Small enough for orbits to close accurately.
2 0. 0. 0. ! Magnet positionning RE, TE, RS, TS. Could be instead non-zero, e.g.,
! 2 RE=50. 0. RS=50. 0., as long as Yo is amended accordingly in OBJET.
'MARKER' #E_180degSectorUnifB ! Label should not exceed 20 characters.
```

2269 3.3 Resonant Acceleration

2270 The field map and TOSCA [16, *lookup* INDEX] model of a 180° sector is used
 2271 here (an arbitrary choice, the analytical field modeling DIPOLE would do as well),
 2272 the configuration is that of Fig. 3.5 with a pair of sectors.

2273 An accelerating gap between the two dees is simulated using CAVITE[IOPT=3],
 2274 PARTICUL is added in the sequence in order to specify ion species and data,
 2275 necessary for CAVITE to operate. Acceleration at the gap does not account for the
 2276 particle arrival time in the IOPT=3 option: whatever the later, CAVITE boost will
 2277 be the same as longitudinal motion is an unnecessary consideration, here).

2278 The input data file for this simulation is given in Tab. 3.8. It is resorted to
 2279 INCLUDE, twice in order to create a double-gap sequence, using the field map model
 2280 of a 180° sector. The INCLUDE inserts the magnet itself, *i.e.*, the #S_halfDipole to
 2281 #E_halfDipole TOSCA segment of the sequence of Tab. 3.3. Note: the theoretical
 2282 field model of Tab. 3.6, segment #S_60degSectorUnifB to #E_60degSectorUnifB
 2283 (to be INCLUDED 3 times, twice), could be used instead: exercise 3.2 has shown
 2284 that both methods, field map and analytical field model, deliver the same results.

2285 Particle data are logged in zgoubi.fai at both occurrences of CAVITE, under the
 2286 effect of FAISTORE[LABEL=cavity], Tab. 3.8. This is necessary in order to access
 2287 the evolution of parameters as velocity, time of flight, etc. at each half-turn, given
 2288 that each half-turn is performed at a different energy

2289 (a) Accelerate a proton.

2290 A proton with initial kinetic energy 20 keV is launched on its closed orbit radius,
 2291 $R_0 = p/qB = 4.087013$ cm. It accelerates over 25 turns due to the presence to
 2292 REBELOTE[NPASS=24], placed at the end of the sequence. The energy range,
 2293 20 keV to 5 MeV, and the acceleration rate: 0.1 MeV per cavity, 0.2 MeV per turn,
 2294 determine the number of turns, $NPASS+1 = (5 - 0.02)/0.2 \approx 25$. The accelerated
 2295 trajectory spirals out in the fixed magnetic field, it is plotted in Fig. 3.26, reading
 2296 data from zgoubi.plt.

Fig. 3.26 Twenty five turn spiral trajectory of a proton accelerated in a uniform 0.5 T field from 20 keV to 5 MeV at a rate of 200 kV per turn (a 100 kV gap voltage). The vertical thick line materializes the gap, the upper half (red) corresponds to the first occurrence of CAVITE in the sequence (Tab. 3.8), the lower half (blue) corresponds to the second occurrence of CAVITE

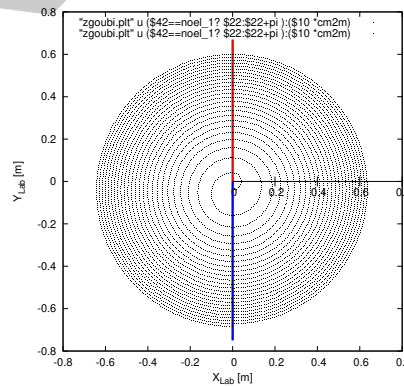


Table 3.8 Simulation input data file: accelerating a proton in a double-dee cyclotron, from 20 keV to 5 MeV, at a rate of 100 kV per gap, independent of RF phase (longitudinal motion is frozen - see question (e) dealing with CAVITE[IOPT=7] for unfrozen motion). Note that particle data are logged in zgoubi.fai (under the effect of FAISTORE) at both occurrences of CAVITE. The INCLUDE file FieldMapSector.inc is taken from Tab. 3.3

```

Cyclotron, classical. Acceleration: 20 keV -> 6 MeV.
'MARKER' ProbAccelGap_S                               ! Just for edition purposes.
'OBJET'
64.62444403717985                                     ! Reference Brho ("BORO" in the users' guide) -> 200keV proton.
2
1 1                                                     ! Just one ion.
4.087013 0. 0. 0. 0. 0.3162126 'o'                   ! D=0.3162126 => Brho[kG.cm]= 20.435064, kin-E[keV]= 20.
1
'PARTICUL'                                             ! Usage of CAVITE requires partical data,
PROTON                                                 ! otherwise, by default \zgoubi\ only requires rigidity.
'FAISTORE'                                             ! Store particle data, turn-by-turn.
zgoubi.fai cavity                                     ! Log coordinates at any occurrence of LABEL=cavity, in zgoubi.fai.
1
'INCLUDE'                                             ! Insert a 180 deg sector field map.
1
FieldMapSector.inc[#S_halfDipole:#E_halfDipole]
'FAISCEAU'                                           ! Particle coordinates before RF gap.
'CAVITE' cavity                                       ! Accelerating gap.
3                                                     ! dW = qVsin(phi), independent of time (phi forced to constant).
0. 0.                                                 ! Unused.
100e3 1.57079632679                                   ! Peak voltage 100 kV; RF phase = pi/2.
'INCLUDE'                                             ! Insert a 180 deg sector field map.
1
FieldMapSector.inc[#S_halfDipole:#E_halfDipole]
'FAISCEAU'                                           ! Particle coordinates before RF gap.
'CAVITE' cavity                                       ! Accelerating gap.
3                                                     ! dW = qVsin(phi), independent of time (phi forced to constant).
0. 0.                                                 ! Unused.
100e3 1.57079632679                                   ! Peak voltage 100 kV; RF phase = pi/2.
'REBELOTE'                                           ! Repeat NPASS=24 times, for a total of 25 turns; K = 99: coordinates at end of
24 0.1 99                                             ! previous pass are used as initial coordinates for the next pass.
'FAISCEAU'                                           ! Local particle coordinates logged in zgoubi.res.

'SYSTEM'
2                                                     ! 2 SYSTEM command follow:
/usr/bin/gnuplot < ./gnuplot_Zplt_XYLab.gnu &         ! plot trajectories;
/usr/bin/gnuplot < ./gnuplot_awk_Zfai_dTT.gnu &       ! dC/C, dbta/bta, dT/T graph.

'MARKER' ProbAccelGap_E                               ! Just for edition purposes.
'END'

```

Two gnuplot scripts, to obtain respectively Fig. 3.26: and Fig. 3.28:

The awk command in gnuplot_awk_Zfai_dTT.gnu takes care of a 1-row shift so to subtract next turn data from currant turn ones.

```

# gnuplot_Zplt_XYLab.gnu
set xtics ; set ytics ; set xlabel "X_{Lab} [m]" ; set ylabel "Y_{Lab} [m]"
set size ratio 1 ; set polar ; cm2m = 0.01 ; pi = 4.*atan(1.)
set arrow from 0, 0 to 0, 0.67 nohead lc "red" lw 6; set arrow from 0, -0.75 to 0, 0 nohead lc "blue" lw 6
noel_1=6 ; noel_2=11 # 1st CAVITE is element noel_1; 2nd CAVITE is noel_2. Col. $42 in zgoubi.plt is element numb.
plot for [nl=noel_1:noel_2:5] "zgoubi.plt" u ($42==noel_1? $22:$22+pi):($10 *cm2m) w p pt 5 ps .2 lc rgb "black"

# gnuplot_awk_Zfai_dTT.gnu
set xtics nomirror; set ytics mirror; set xlabel "E_k [MeV]";
set ylabel "{/Symbol Db}/{/Symbol b}, {/Symbol D}C/C, {/Symbol D}T_{rev}/T_{rev}"; set logscale y; set yrange [:3]
# zgoubi.fai columns: $25: energy; $14: path length; $23: kinetic E; $29: mass; $15: tim
plot "< awk '/#/{next}; { if(prev14>0 && prev25>0) print prev24, ($14 -prev14)/prev14 , prev24} \
{ prev14 = $14; prev24 = $24; prev25=$25 }' < zgoubi.fai" u 1:2 w p pt 5 lc rgb "black" tit "{/Symbol D}C/C" , \
"< awk '/#/{next}; { if(prev14>0 && prev25>0) print prev24, (-sqrt(prev25**2-$29**2)/prev25 + \
sqrt($25**2-$29**2)/$25 )/(sqrt(prev25**2-$29**2)/prev25) , prev24} { prev14 = $14; prev24 = $24; prev25=$25 }' \
< zgoubi.fai" u 1:2 w p pt 6 ps 1.5 lc rgb "red" tit "d{/Symbol b}/{/Symbol b}" , \
"< awk '/#/{next}; { if(prev14>0 && prev25>0) print prev24, ($14 -prev14)/prev14- (-sqrt(prev25**2-$29**2)/prev25 \
+ sqrt($25**2-$29**2)/$25 )/(sqrt(prev25**2-$29**2)/prev25) , prev24} { prev14 = $14; prev24 = $24; prev25=$25 }' \
< zgoubi.fai" u 1:2 w p pt 8 ps 1.5 lc rgb "blue" tit "{/Symbol D}T/T=dC/C-d{/Symbol b}/{/Symbol b}" , \
"< awk '/#/{next}; { if(prev14>0 && prev15>0) print prev24, ($15-prev15)/prev15 , prev24} { prev14 = $14; \
prev24 = $24; prev15=$15 }' < zgoubi.fai" w l lw 2 lc rgb "blue" tit "theor. {/Symbol D}T/T"

```


2297 (b) Momentum and energy.

2298 Proton momentum p and total energy E as a function of kinetic energy, from
 2299 raytracing (turn-by-turn particle data are read from `zgoubi.fai`, filled up due to FAI-
 2300 STORE) are displayed in Fig. 3.27, together with theoretical expectations, namely,
 2301 $p(E_k) = \sqrt{E_k(E_k + 2M)}$ and $E = E_k + M$.

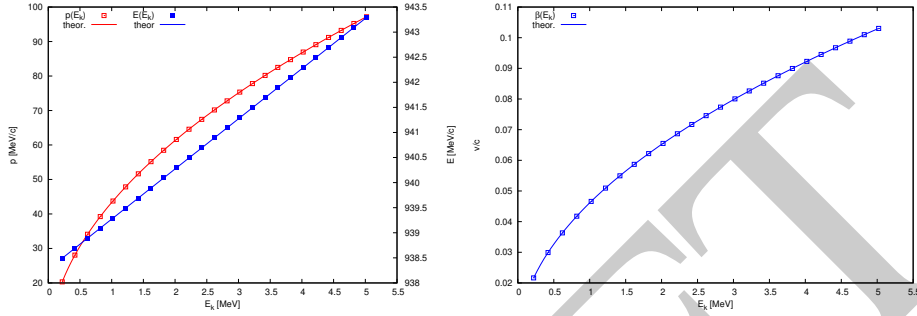
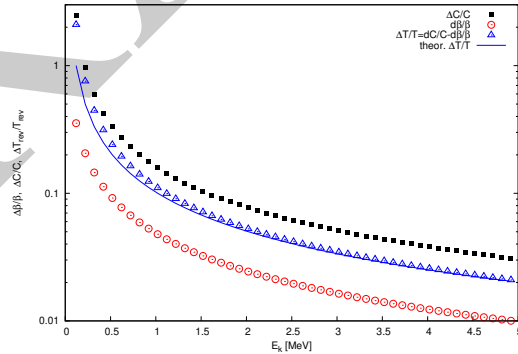


Fig. 3.27 Energy dependence of, left: proton momentum p (left axis) and total energy E (right axis) and of, right: proton normalized velocity $\beta = v/c$. Markers: from raytracing; solid lines: theoretical expectation

2302 (c) Velocity.

2303 Proton normalized velocity $\beta = v/c$ as a function of kinetic energy from raytracing
 2304 is displayed in Fig. 3.27, together with theoretical expectation, namely, $\beta(E_k) =$
 2305 $p/(E_k + M)$.

Fig. 3.28 Relative variation of velocity $\Delta\beta/\beta$ (empty circles), circumference $\Delta C/C$ (solid disks) and revolution time $\Delta T/T$ (triangles), as a function of energy, from raytracing. Theoretical expectation for the latter is also displayed (solid line), for comparison



2306 (d) Relative velocity, orbit length and time of flight.

2307 The relative increase in velocity is smaller than the relative increase in orbit length
 2308 as energy increases (this is what Fig. 3.28 shows). Thus the relative variation of the

2309 revolution time, Eq. 3.23, is positive; in other words the revolution time increases
 2310 with energy, the revolution frequency decreases. Raytracing outcomes are displayed
 2311 in Fig. 3.28, they are obtained using the gnuplot script given in Tab. 3.8. Note that
 2312 the path length difference (taken as the difference of homologous quantities in a
 2313 common line) is always between the two CAVITEs (particle data are logged at the
 2314 two occurrences of CAVITE), crossed successively, which is half a turn. Same for
 2315 the difference between homologous velocity data on a common line, it corresponds
 2316 to two successive crossings of CAVITE, *i.e.*, half a turn. The graph includes the
 2317 theoretical $\delta T_{\text{rev}}/T_{\text{rev}}$ (Eq. 3.23) for comparison with raytracing; some difference
 2318 appears in the low velocity regime, this may be due to the large $\Delta\beta$ step imparted by
 2319 the 100 kV acceleration at the gaps.

2320 (e) Harmonic $h=3$ RF.

2321 The input data file for this simulation is given in Tab. 3.9. The RF is on harmonic
 2322 $h=3$ of the revolution frequency. It has been tuned to ensure acceleration up to 3 MeV.
 2323 The accelerating gap between the two dees is simulated using CAVITE[IOPT=7]: by
 2324 contrast with the previous exercise (where CAVITE[IOPT=3] is used), the RF phase
 2325 at ion arrival at the gap is now accounted for.

Table 3.9 Simulation input data file: accelerating a proton in a double-dee cyclotron, from 20 keV to 5 MeV, using harmonic 3 RF. The INCLUDE file is taken from Tab. 3.6

```

Cyclotron, classical. Analytical model of dipole field.
'OBJET'
64.62444403717985                                ! 200keV proton.
2
1 1                                                ! Just one ion.
12.924888 0. 0. 0. 1. 'm'                        ! D=1 => 200keV proton. R=Brho/B=64.624444037 [KG.cm]/5 [KG].
1
'PARTICUL'                                       ! This is required for spin motion to be computed,
PROTON                                           ! otherwise, by default \zgoubi\ only requires rigidity.
'INCLUDE'
1                                                ! Include a first 180 deg sector.
./180degSector.inc[#S_180degSectorUnifB:#E_180degSectorUnifB]
'CAVITE'
7
0 22862934.0
285e3 -0.5235987755982988
'INCLUDE'
1                                                ! Include a second 180 deg sector.
./180degSector.inc[#S_180degSectorUnifB:#E_180degSectorUnifB]
'CAVITE'
7
0 22862934.0                                       ! RF = 3/T_rev.
285e3 -3.665191429188092                          ! Peak voltage; synchronous phase.
'REBELOTE'
26 0.4 99                                         ! 26+1 turn tracking.
'END'

```

2326 Repeating questions (b-d) is straightforward, changing what needs be changed in
 2327 Tab. 3.9 input data file.